Large-Scale Fading Characterization in Curved Modern Subway Tunnels

Ke Guan , Bo Ai , Zhangdui Zhong , Carlos F. López , Lei Zhang , Cesar Briso-Rodríguez , and Bei Zhang

***Abstract*—This paper presents extensive propagation measurements conducted in a modern arched tunnel with 300 m and 500 m radii of curvature with horizontal polarizations at 920 MHz, 2400 MHz, and 5705 MHz, respectively. Based on the measurements, statistical metrics of propagation loss and shadow fading in all the measurement cases are extracted. Furthermore, for each of the large-scale fading parameters, extensive analysis and discussions are made to reveal the physical laws behind the observations. The quantitative results and findings are useful to realize intelligent transportation systems in the subway system.**

I. Introduction

Various kinds of wireless communication techniques employed for subway system play a critical role to ensure personnel safety and enhance operational efficiency. No matter for public wireless communication systems or signaling and train control communication systems, 900 MHz, 2400 MHz, and 5800 MHz are three "hot" frequency bands. Thus, both industry and academia have great interest at the information on propagation characteristics in these three frequency bands. At 5800 MHz, there are many wireless radio system deployments based on WLAN (wireless local area network) to realize driverless underground systems, such as in New-York, line 1 in Paris, Malaga, Marmaray, Singapore, etc. At 2400 MHz frequency band, there are Wi-Fi (Wireless Fidelity), UMTS (Universal Mobile Telecommunications System), LTE, CBTC (Communication Based Train Control System), and LTE-R (pending). At 900 MHz frequency band, there are GSM (Global System for Mobile Communications), GSM-R (Global System for Mobile Communications for Railway), LTE (Long Term Evolution), TETRA (Terrestrial Trunked Radio), and LTE-R (Long Term Evolution for Railway).

In order to predict the radio coverage of these wireless communication systems in subway tunnels, numerical investigations on propagation of UHF (ultra-high frequency: 300 MHz–3 GHz) and SHF (super high frequency: 3 GHz–30 GHz) signals in tunnels have been done in the last decades. For the measurements, authors of [1]–[3] reported the measurement results of propagation characteristics in tunnels, railway and road tunnels, and subway tunnels, respectively. For the modeling methodologies, many researchers proposed modal analysis based on waveguide theory [4], models based on geometrical optics (GO) approach [5], numerical models based on vector parabolic equation (VPE) techniques [6], and empirical models based on measurements (two-slope models [7], three-slope model [8], four-slope model [2], five-zone models [9], etc.). Both these experimental and theoretical studies form the understanding of wave propagation inside tunnels. However, most of them focus on the straight tunnels. Research on the propagation in curved tunnels are still limited. Authors of [10] developed simulators based on ray approaches for the wave propagation in curved tunnels with some specific cross sections. Authors of [11] simulated the propagation loss in curved tunnels with modal analysis. Authors of [12] predicted the loss for curved tunnels by using the parabolic equation (PE) along with the alternate direction implicit (ADI) method. To sum up, most of the existing research on the tunnel curve make the contributions on modeling and simulation methods, the measurement results focus on road, mine, and railway tunnels with specific cross sections. The measurement results in the curved subway tunnels (which are much smaller than road and railway tunnels, and are different from mine tunnels) are still rarely presented. This limits the validation of the corresponding simulators and the deployment of wireless communication systems in subway systems.

This paper presents a sets of measurements on wave propagation in a typical modern curved subway tunnel. The extracted large-scale fading characterization supplies the first-hand information, and can be used for network planning, channel modeling, key techniques (such as soft handover, link adaptation, etc.) evaluation, and validation for simulators of different communication systems deployed in tunnel environment at various frequencies.

The rest of this paper is organized as follows. The measurement campaign is described in Section II. The measurements are made in a modern curved arched tunnel. The radii of curvature are 300 m and 500 m, which are the typical values of subway tunnels. Corresponding to the three hot frequency bands, frequencies at 920 MHz, 2400 MHz, and 5705 MHz with horizontal polarization are tested in the measurements. In Section III, methods of extracting large-scale fading parameters (path loss exponent, shadow fading

This work is supported by the NNSF of China under Grant U1334202, 863 project under Grant 2014AA01A706, NNSF under Grant 61222105, the Fundamental Research Funds for the Central Universities (No. 2014RC018), and State Key Lab of Rail Traffic Control and Safety Project under Grant RCS2014ZT11 and RCS2014ZT32, and being developed under the framework of INNPACTO TECRAIL research project IPT-2011-1034-37000 funded by the Spanish Ministry of Economy and Competitiveness.

distribution, autocorrelation, and cross-correlation) from measurement results are introduced. In Section IV, the large-scale fading characteristics of wave propagation in the curved arched tunnel are quantitatively analyzed, and finally summarized in a series of tables. Conclusions are drawn in Section V.

II. Measurement Campaign

A. Test system

The test system is composed of two parts as follows:

1) Transmitting system: The transmitting system is comprised of a continuous wave (CW) transmitter (Tx) and a panel antenna. Since totaly three distinguished interesting frequencies are measured, three transmitters and corresponding antennas are utilized. For the measurements at 920 MHz, a Tx with 500 mW (27 dBm) power output, and a L-COM HG908 panel antenna working at the frequency band 902-928 MHz, with 8 dBi gain, 75° horizontal and 65° vertical beam widths are used. In the measurements at 2400 MHz, a Tx with 250 mW (24 dBm) power output is employed to be the Tx; a L-COM HG2414P panel antenna working at the frequency band 2400-2500 MHz, with 14 dBi gain, 30° horizontal and 30° vertical beam widths is utilized. In the cases of 5705 MHz, the Tx is a transmitter with 160 mW (22 dBm) power output; the antenna is a L-COM HG5419P panel antenna working at the frequency band 5470-5850 MHz, with 19 dBi gain, 16° horizontal and 16° vertical beam widths. In order to avoid possible damage in the measurements, the transmitting system is attached to a pylon located on land.
2) Receiving system: The receiving system is composed of a broadband antenna, an amplifier, and a spectrum analyzer, located on a standard subway train. The receiving antenna is an R&S HL050 Log-Periodic WB antenna, with 8.5 dBi gain, 85° horizontal and 70° vertical beam widths, located in the front car of the train (see Fig. 1). A Celwritek csa-936327 (teledyne) amplifier working at the frequency band 500-6000 MHz is used to amplify the received power. An Agilent N9912A spectrum analyzer is employed to send the captured received signal power to a laptop, stored for the later processing.

In the measurements, the sampling intervals are shorter than one wavelength, and repeated measurements are taken to collect sufficient samples for study of the fading behavior. Since this study focuses on the large-scale fading property specified in real curved arched tunnels, the small-scale fading is separated from the received power by averaging samples at intervals of 40 wavelengths. The lowest average signal-to-noise-ratio (SNR) measured at a particular location is approximately 30 dB so that an accurate estimation of channel parameters is possible.

B. Measurement environment

The measurements are conducted in a modern arched curved tunnel of Madrid's subway. As shown in Fig. 1, the tunnel includes arched walls and roof, and a plane floor, which is common in the newly built subway lines, because of the widespread use of the shield machines in the constructions of modern tunnels. Relative position and configuration of the transmission system and receiving system along the train route inside the arched tunnel with dimensions 8.41 m $\times$ 6.87 m are illustrated in Fig. 1 as well. Positions of Tx and Rx as well as the radii of curvature of the tunnel are given by Table I. Three carrier frequencies – 920 MHz, 2400 MHz, and 5705 MHz – are used in the measurements. In the curved arched tunnel, two radii of curvature (300 m and 500 m) are tested at the three frequencies with horizontal polarization (H-pol.). Horizontal polarization is chosen to study because it is more sensitive to the tunnel curve than vertical polarization.

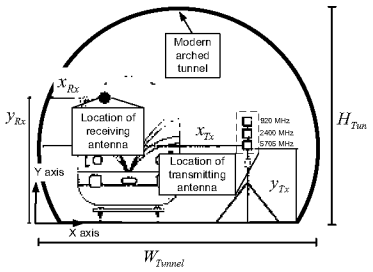

Fig. 1. Front view of measurement setup in the arched tunnel

III. Measurement Results and Parameter Extraction

A. Received power in the curved arched tunnels

The received power in the measurement campaigns are shown in Fig. 2. Some preliminary observations on the influences of the following factors could be summarized:

1) Frequency: when the other factors (polarization, tunnel, radius of curvature) are the same, wave propagation at the three frequencies suffers similar loss. In the straight tunnel, the waveguide theory suggests that the wave at higher frequencies experiences the smaller propagation loss. Thus, the fact that the total losses at various frequencies are similar in the measurements, virtually implies that the higher frequencies are more sensitive to the tunnel curve. In terms of the fading, the case in the curved tunnel follows the same law in the straight tunnel: higher frequencies have stronger fading.
2) Radius of curvature: in the arched tunnel with horizontal polarization, the wave suffers larger propagation loss with the 300 m radius of curvature than that of the 500 m radius of curvature. This follows the common sense that the sharper curve leads to larger propagation loss. Similar results are reported by [10], [12].

These observations justify the measurement data, and imply the factors behind the propagation loss in the curved tunnels.

B. Path loss exponent and shadow fading extraction

In the log-distance path loss model, the change of the path loss along with the distance is depicted by the path loss

TABLE I
POSITIONS OF TX AND RX IN THE MEASUREMENTS

Tunnel	W_{Tunnel} (m)	H_{Tunnel} (m)	x_{Tx} (m)	y_{Tx} (m)	x_{Rx} (m)	y_{Rx} (m)	Radius of Curvature (m)
Arched	8.41	6.87	6.75	2.15	1.7	2.84	300 and 500

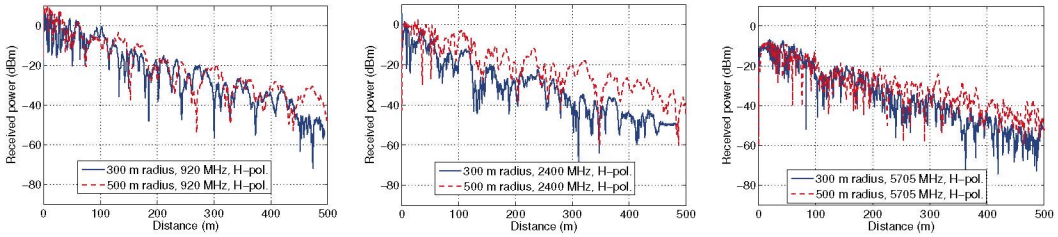

(a) (b) (c)

Fig. 2. Measured received power (without small-scale fading) in the modern curved arched tunnel with 300 m and 500 m radii of curvature with horizontal polarization at (a) 920 MHz, (b) 2400 MHz, and (c) 5705 MHz.

exponent. Such exponent and shadow fading are extracted from the measured results by using the following expression:

$$L(d) = \overline{L}(d_0) + 10n \lg\left(\frac{d}{d_0}\right) + X_\sigma \tag{1}$$

where d denotes the distance (along the track of the tunnel) between Tx and Rx. $L(d)$ denotes the propagation loss without small-scale fading. d_0 denotes the referenced distance. $\overline{L}(d_0)$ denotes the media path loss at d_0. n denotes the path loss exponent. X_σ denotes the shadow fading. By using the least-square criterion, the path loss exponent n can be obtained. The shadow fading values can be calculated by using a simple minus to the formula offered above.

C. Amplitude distribution of shadow fading

In extensive literature, the log-normal distribution has been empirically confirmed for fitting the amplitude distribution of shadow fading. In this study, the shadow fading is well fitted by the log-normal distribution as well, passing Kolmogorov-Smirnov, Anderson-Darling, and Chi-Squared tests in Easy Fit [13]. The shadow fading standard deviations (σ) based on the averaging of repeated measurements are given by Table II.

D. Autocorrelation calculation

Besides the distribution, another important characteristic of the shadow fading is the autocorrelation, and it is of interest for power control and base station (or access point) location designing. This metric is defined as the correlation of shadow fading in different positions of the signal from the same Tx. The autocorrelation is described by the correlation coefficient in numerical documents with the following definitions:

$$\rho_{1,2} = \frac{\mathrm{E}\{S(d_1)\,S(d_2)\}}{\sigma(d_1)\,\sigma(d_2)} \tag{2}$$

where $S(d_1)$ denotes the value of shadow fading in the position with distance d_1; $S(d_2)$ denotes the value of shadow fading in the position with distance d_2. $\sigma(d_1)$ and $\sigma(d_2)$ denote the standard deviations of the shadow fading in the positions with distance d_1 and d_2, respectively. There are mainly two definitions for such decorrelation distance. The first one – $d_{cor}(0.5)$ – is defined as the distance that the correlation is equal to 0.5. The other definition – $d_{cor}(e^{-1})$ – is the distance when the correlation is equal to e^{-1}.In order to provide a general reference, both definitions of decorrelation distance are calculated by using least squares (LS) fitting based on the repeated measurement results.

E. Cross-correlation calculation

The cross-correlation is extracted from the measurement results as well. This metric is of interested in designing handover algorithms, controlling interference power, and so on. The shadow fading cross-correlation coefficient ρ is defined as the cross-correlation coefficient between shadow fading components of two sets of received signals, by using the following expression:

$$\rho = \frac{\sum_{i=1}^{n}(X_i - \overline{X})(Y_i - \overline{Y})}{\sqrt{\sum_{i=1}^{n}(X_i - \overline{X})^2}\sqrt{\sum_{i=1}^{n}(Y_i - \overline{Y})^2}}, \tag{3}$$

where X_i and Y_i denote the shadow fading components of two separate received power, $\overline{X}$ and $\overline{Y}$ are the mean of shadow fading components, n is the number of the shadow fading component samples. In this paper, n ranges from 200 to 400 in different measurement routes. Usually, if the absolute value of the estimated correlation coefficient lies in $[0, 0.1]$, two random variables can be treated as uncorrelated. In this study, the cross-correlation coefficients of shadow fading between different frequencies are evaluated from the measurements.

IV. ANALYSIS AND DISCUSSION

Based on the parameter extraction from the measurement results, the large-scale fading characteristics of wave propa-

gation in the curved arched tunnel are quantitatively analyzed and discussed in this section.

A. Path loss exponent and shadow fading distribution in the curved arched tunnel

Table II shows the path loss exponents as well as shadow fading distributions and standard deviations (Std) in the curved arched tunnel with various frequencies and radii of curvature. More comparisons of these characteristics between various straight and curved tunnels are discussed detailedly in [14]. From Table II, following findings can be summarized:

1) Most of the path loss exponents are larger than 2 (which equals the case of free-space propagation), and much larger than the cases of the straight tunnels where the waveguide effect is established (see the comparison in [14]). This implies that the tunnel curve reduces the waveguide effect, and leads to the extra loss of propagation compared to the cases of the straight tunnels.
2) In Table II, the path loss exponents of the horizontal polarized wave propagation in the arched tunnel with 300 m radius of curvature are between 4.61 and 5.50, which are larger than the values (3.36-5.37) with 500 m radius of curvature. This means that the sharper the tunnel curve is, the larger the path loss is. Similar conclusions can be found in [11].
3) The path loss exponents at 2400 MHz and 5705 MHz are close to each other, and are obviously larger than those at 920 MHz. Note that the exponents at 2400 MHz are slightly larger than 5705 MHz may be due to specificity or uncertainty of measurements, and therefore, is not discussed here. Given the fact that the higher frequencies suffer smaller path loss in the straight tunnels, it could be concluded that the higher frequencies are more sensitive to the tunnel curve. In a more extreme case presented by [15], the path loss could even ascend along with the increase of frequency in curved tunnels.
4) The standard deviations of the shadow fading are from 4.09 dB to 6.52 dB in the curved arched tunnel. These values are larger than the standard deviations of the shadow fading in the other railway scenarios, such as train station, cutting, and viaduct.

B. Autocorrelation characteristics of shadow fading in the curved arched tunnel

Table III gives the statistics of the decorrelation distances in the curved arched tunnel with two definitions of the decorrelation distances, various frequencies and radii of curvature, respectively. The decorrelation distances defined as $d_{cor}\left(0.5\right)$ are shorter than the values of the definition of $d_{cor}\left(e^{-1}\right)$. When the radius of curvature is 500 m, the mean values of decorrelation distances are 11.19-16.75 m, 1.41-1.83 m, and 4.13-5.78 m, at 920 MHz, 2400 MHz, and 5705 MHz, respectively. Most of these values are larger than the corresponding values when the radius of curvature is 300 m. This suggests that the sharper curve favors the decorrelation of the received signal. The decorrelation distances in the curved tunnel are much shorter than those in the urban macro environments (32 m, 45 m, and 97 m) [16] as well as other outdoor rail traffic scenarios, such as viaduct (14.81-131.6 m) [17], [18]. This indicates that compared with the open space, the shadow fading component along the distance varies faster in the curved confined space, e.g., the curved subway tunnels in this study. This means that the propagation inside curved tunnels needs special attention for communication system design.

C. Cross-correlation characteristics of shadow fading in the curved arched tunnel

Cross-correlation characteristics of shadow fading in the curved tunnel between various measurement configurations are shown in Table IV. The shadowing cross-correlation in the sharper curve (300 m radius of curvature) tends to be weaker than that of the gentle curve (500 m radius of curvature), but the difference is not substantial, and the case of the "920 MHz vs 5705 MHz" is an exception. It indicates that the variation of curved radius in the tunnel has little impact on shadowing cross-correlation. Based on these results, frequency diversity between the three bands (920 MHz, 2400 MHz, and 5705 MHz) holds promise for diversity gains since the channel effects in these three bands are essentially uncorrelated. In other words, various communication systems at 900 MHz frequency band (GSM/GSM-R/LTE/TETRA/LTE-R), 2400 MHz frequency band (Wi-Fi/UMTS/LTE/CBTC/LTE-R), and 5800 MHz (CBTC, custom systems, etc), are promising to work together in the same curved tunnel without severe interference.

V. Conclusion

A set of propagation measurements are conducted in a modern arched subway tunnel with 300 m and 500 m radii of curvature, horizontal polarization, at 920 MHz, 2400 MHz, and 5705 MHz, respectively. In terms of the path loss, the fact that most of the path loss exponents are larger than 2, reflects that the tunnel curve indeed reduces the waveguide effect, so that the wave propagation suffers much larger loss than the cases of the straight tunnels. Meanwhile, the measurement results indicates that the sharper the tunnel curve is, the larger the path loss is. Moreover, it is found that the higher frequencies are more sensitive to the tunnel curve. In terms of the shadow fading distribution, the measured shadow fading can be well fitted by the log-normal distribution, with the standard deviations from 4.09 dB to 6.52 dB in the curved arched tunnel. For the autocorrelation and decorrelation distance, the mean values of decorrelation distances are several meters, much shorter than those in the urban macro environments or other outdoor rail traffic scenarios. In terms of the cross-correlation of shadow fading, the signals in different frequencies are uncorrelated. This gives the chance to employ the frequency diversity to ensure reliable communication in subway systems for emergency cases. Moreover, various communication systems at various frequency bands are expected to work simultaneously in the same curved tunnel without severe interference.

References

[1] D. Dudley, M. Lienard, S. Mahmoud, and P. Degauque, "Wireless propagation in tunnels," *IEEE Antennas and Propagation Magazine*, vol. 49, no. 2, pp. 11–26, April 2007.

TABLE II
PATH LOSS EXPONENT AND SHADOW FADING IN THE CURVED ARCHED TUNNEL

Tunnel:	Modern Arched			Polarization:		Horizontal
Radius of Curvature	500 m			300 m		
Frequency	920 MHz	2400 MHz	5705 MHz	920 MHz	2400 MHz	5705 MHz
Path Loss Exponent	3.36	5.37	4.94	4.61	5.50	4.78
Shadow Fading	Log-Normal Distribution					
Std	6.52 dB	4.67 dB	4.46 dB	4.64 dB	4.09 dB	5.18 dB

TABLE III
DECORRELATION DISTANCE STATISTIC IN THE CURVED ARCHED TUNNEL

Tunnel:	Modern Arched;						Polarization:		Horizontal			
Radius of Curvature	300 m						500 m					
Frequency	920 MHz		2400 MHz		5705 MHz		920 MHz		2400 MHz		5705 MHz	
Decorrelation Distance [m]	$d(0.5)$	$d(e^{-1})$	$d(0.5)$	$d(e^{-1})$	$d(0.5)$	$d(e^{-1})$	$d(0.5)$	$d(e^{-1})$	$d(0.5)$	$d(e^{-1})$	$d(0.5)$	$d(e^{-1})$
10%	3.89	5.30	1.59	1.86	2.96	2.96	9.83	10.50	0.73	0.73	2.96	4.00
50%	5.74	6.67	1.86	2.33	2.96	3.44	10.50	11.38	0.73	2.66	4.00	4.84
90%	8.79	11.50	2.80	3.30	3.44	9.18	11.08	37.77	2.66	2.66	4.84	6.60
Mean	6.35	8.87	2.05	2.56	3.23	5.50	11.19	16.75	1.41	1.83	4.13	5.78

TABLE IV
CROSS-CORRELATION OF THE SHADOW FADING BETWEEN THE 920 MHZ, 2400 MHZ, AND 5705 MHZ IN THE CURVED SUBWAY TUNNEL

Tunnel:	Modern Arched		Polarization: Horizontal
Frequency Bands	920 MHz vs 2400 MHz	920 MHz vs 5705 MHz	2400 MHz vs 5705 MHz
Radius: 300 m	0.23	0.12	0.04
Radius: 500 m	0.27	0.04	0.07

[2] A. Hrovat, G. Kandus, and T. Javornik, "Four-slope channel model for path loss prediction in tunnels at 400 MHz," *IET Microwaves, Antennas and Propagation*, vol. 4, no. 5, pp. 571–582, May 2010.

[3] K. Guan, Z. Zhong, J. I. Alonso, and C. Briso, "Measurement of distributed antenna systems at 2.4 GHz in a realistic subway tunnel environment," *IEEE Transactions on Vehicular Technology*, vol. 61, no. 2, pp. 834–837, Feb. 2012.

[4] K. Guan, Z. Zhong, B. Ai, and C. Briso, "Proc. propagation mechanism analysis before the break point inside tunnels," in *IEEE 74th Veh. Technol. Conf.*, San Francisco, CA, USA, 2011, pp. 1–5.

[5] F. Pallares, F. Juan, and L. Juan-Llacer, "Analysis of path loss and delay spread at 900 MHz and 2.1 GHz while entering tunnels," *IEEE Transactions on Vehicular Technology*, vol. 50, no. 3, pp. 767–776, May 2001.

[6] A. V. Popov and N. Y. Zhu, "Modeling radio wave propagation in tunnels with a vectorial parabolic equation," *IEEE Transactions on Antennas and Propagation*, vol. 48, no. 9, pp. 1403–1412, Sep. 2000.

[7] Y. Zhang, "Novel model for propagation loss prediction in tunnels," *IEEE Transactions on Vehicular Technology*, vol. 52, no. 5, pp. 1308–1314, Sep. 2003.

[8] K. Guan, Z. Zhong, B. Ai, R. He, Y. Li, and C. Briso, "Propagation mechanism modeling in the near-region of arbitrary cross-sectional tunnels," *International Journal of Antennas and Propagation*, vol. 2012, p. 11, 2012. [Online]. Available: http://dx.doi.org/10.1155/2012/183145

[9] K. Guan, Z. Zhong, B. Ai, R. He, B. Chen, Y. Li, and C. Briso, "Complete propagation model in tunnels," *IEEE Antennas and Wireless Propagation Letters*, vol. 12, pp. 741–744, Jul. 2013.

[10] E. Masson, Y. Cocheril, P. Combeau, L. Aveneau, M. Berbineau, R. Vauzelle, and E. Fayt, "Radio wave propagation in curved rectangular tunnels at 5.8 GHz for metro applications," in *Pro. 11th International Conference on ITS Telecommunications (ITST)*, St. Petersburg, Russia, 2011, pp. 81–85.

[11] Y. Zhang, Y. Hwang, and P. Ching, "Characterization of UHF radio propagation channel in curved tunnels," in *Proc. Seventh IEEE International Symposium on Personal, Indoor and Mobile Radio Communications, PIMRC'96.*, vol. 3, Taipei, 1996, pp. 798–802.

[12] R. Martelly and R. Janaswamy, "Modeling radio transmission loss in curved, branched and rough-walled tunnels with the ADI-PE method," *IEEE Transactions on Antennas and Propagation*, vol. 58, no. 6, pp. 2037–2045, 2010.

[13] K. Schittkowski, "EASY-FIT: a software system for data fitting in dynamical systems," *Structural and Multidisciplinary Optimization*, vol. 23, no. 2, pp. 153–169, Mar. 2002.

[14] K. Guan, B. Ai, Z. Zhong, C. F. López, L. Zhang, C. Briso, A. Hrovat, B. Zhang, R. He, and T. Tang, "Measurements and analysis of large-scale fading characteristics in curved subway tunnels at 920 mhz, 2400 mhz, and 5705 mhz," *IEEE Transactions on Intelligent Transportation Systems*, to appear 2015.

[15] J. Sun and C. Zhang, "Analysis of transmission characteristics of curved tunnel with arbitrary cross section using hybrid mode matching/finite elements approach," in *Proc. IEEE International Symposium on Communications and Information Technology*, vol. 1, 2005, pp. 63–66.

[16] Y. Zhang, J. Zhang, D. Dong, X. Nie, G. Liu, and P. Zhang, "A novel spatial autocorrelation model of shadow fading in urban macro environments," in *Proc. IEEE Global Telecommunications Conference*, New Orleans, LO, USA, Nov. 2008, pp. 1–5.

[17] F. Luan, Y. Zhang, L. Xiao, C. Zhou, and S. Zhou, "Fading characteristics of wireless channel on high-speed railway in hilly terrain scenario," *International Journal of Antennas and Propagation*, vol. 2013, p. 9, 2013. [Online]. Available: http://dx.doi.org/10.1155/2013/378407

[18] H. Wei, Z. Zhong, L. Xiong, B. Ai, and R. He, "Study on the shadow fading characteristic in viaduct scenario of the high-speed railway," in *Proc. 6th International ICST Conference on Communications and Networking in China (CHINACOM)*, Harbin, China, Aug. 2011, pp. 1216–1220.